Inorganic Chemistry

Article

pubs.acs.org/IC

High-Pressure Synthesis, Structure, and Photoluminescence of a New $KSbO_3$-Type Bismuth Germanate $Bi_3Ge_3O_{10.5}$

Jinguang Cheng,*[,†,▽] Alexander J. E. Rettie,[‡] Matthew R. Suchomel,[§] Haidong Zhou,[∥] Jiaqiang Yan,[⊥,#] Jie Song,[†] Luke G. Marshall,[†] Sebastian A. Larregola,[†] Jianshi Zhou,*[,†] and John B. Goodenough[†]

[†]Materials Science and Engineering Program/Mechanical Engineering, University of Texas at Austin, Austin, Texas 78712, United States

[‡]Department of Chemical Engineering, University of Texas at Austin, Austin, Texas 78712, United States

[§]Advanced Photon Source, Argonne National Laboratory, Argonne, Illinois 60439, United States

[∥]Department of Physics and Astronomy, University of Tennessee, Knoxville, Tennessee 37996, United States

[⊥]Materials Science and Technology Division, Oak Ridge National Laboratory, Oak Ridge, Tennessee 37831, United States

[#]Department of Materials Science and Engineering, University of Tennessee, Knoxville, Tennessee 37996, United States

Supporting Information

ABSTRACT: A new $Bi_3Ge_3O_{10.5}$ compound has been synthesized under high pressure, P = 7 GPa, and 700 °C. Instead of the pyrochlore that is normally stabilized under high pressure, the $Bi_3Ge_3O_{10.5}$ crystallizes in a $KSbO_3$-ype crystal structure. The crystal structure has been refined by the Rietveld method from synchrotron X-ray diffraction data. Moreover, we have also characterized the $Bi_3Ge_3O_{10.5}$ by X-ray photoelectron spectroscopy, photoluminescence, and specific heat.

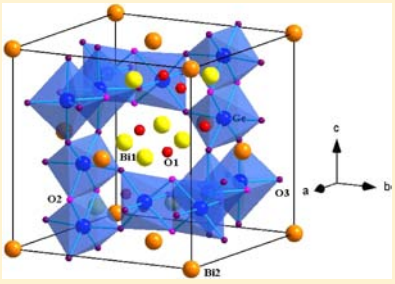

INTRODUCTION

The phase equilibrium of the binary system Bi_2O_3−GeO_2 at ambient pressure has been extensively investigated since the 1960s with several compounds identified in the phase diagram, including three stable compounds, $Bi_2Ge_3O_9$, $Bi_4Ge_3O_{12}$, and $Bi_{12}GeO_{20}$, and two metastable compounds, Bi_2GeO_5 and Bi_4GeO_8.[1,2] Among these compounds, the cubic $Bi_4Ge_3O_{12}$[3,4] and $Bi_{12}GeO_{20}$[5] are known as good oxide-based scintillator materials and have a wide range of applications in high-energy physics, aerospace physics, nuclear medicine, geology exploration, and other industries. Large $Bi_4Ge_3O_{12}$ single crystals grown with the Czochralski method are commercially available. Under high-pressure conditions, we can expand the phase equilibrium of the binary system Bi_2O_3−GeO_2. In this communication, we report the high-pressure synthesis, crystal structure, and photoluminescence of a new $KSbO_3$-type bismuth germanate $Bi_3Ge_3O_{10.5}$.

EXPERIMENTAL PROCEDURE

Polycrystalline $Bi_3Ge_3O_{10.5}$ samples were obtained via solid-state reaction of a stoichiometric mixture of Bi_2O_3 and GeO_2 at 7 GPa and 700 °C for 30 min in a Pt capsule. The product was quenched to room temperature before releasing pressure. The high-pressure and high-temperature (HPHT) synthesis was performed by using a Walker-type multianvil module (Rockland Research Co.). Details about the sample assembly for HPHT synthesis can be found elsewhere.[6] The high-pressure product was first checked by the powder X-ray diffraction (XRD) at room temperature with a Philips X'pert diffractometer (Cu Kα radiation). High-resolution diffraction data have been collected at room temperature with synchrotron radiation on beamline 11-BM (λ = 0.413 034 Å) at the Advanced Photon Source, Argonne National Laboratory.[7] The powder sample was loaded into a 0.3 mm diameter glass capillary, which spins at ~60 Hz during data collection. The obtained synchrotron X-ray diffraction (SXRD) data were analyzed with the Rietveld method with the EXPGUI program.[8] An X-ray absorption coefficient μ_r = 4.50 (estimated by assuming a 0.6 packing fraction) was included in the Rietveld analysis. Diffuse reflectance UV−vis spectra were measured with a Cary 500 spectrophotometer attached to an integrating sphere (Labsphere DRA-CA-5500). Photoluminescence spectroscopy was performed at room temperature with a Fluorolog-3 spectrofluorometer (Horiba Scientific). Spectra were corrected for the features of the Xe lamp and photodetector. The morphology and cation ratio were measured with a scanning electron microscope (SEM, JEOL JSM-5610) equipped with an energy-dispersive spectroscope (EDS). The average Bi:Ge ratio of randomly selected spots on the high-pressure product is 1.035. X-ray photoelectron spectroscopy (XPS) data were acquired with a Kratos AXIS 165 Multitechnique Electron Spectrometer with a monochromatic Al Kα (1486.6 eV) source (Manchester, U.K.). The specific heat was measured from 2 to 200 K with a commercial Physical Property Measurement System (PPMS, Quantum Design).

Received: November 20, 2012
Published: January 27, 2013

   dx.doi.org/10.1021/ic3024277 | Inorg. Chem. 2013, 52, 2138−2141

RESULTS AND DISCUSSION

It is well-known that the stability of the $A_2B_2O_7$ pyrochlore structure depends upon the ratio of the ionic radii, $\rho = r_A/r_B$, which has an upper limit of 1.55 at ambient pressure.[9] Previous high-pressure studies have shown that the upper limit of ρ can be extended significantly up to 1.98 in $In_2Si_2O_7$ by the application of high pressure.[10] In an attempt to synthesize the "$Bi_2Ge_2O_7$" pyrochlore with a ρ = 1.94 under HPHT conditions, we found that the powder XRD pattern of the recovered high-pressure product does not confirm the formation of the cubic pyrochlore structure as other $R_2Ge_2O_7$ (e.g., R = Ho) in Figure 1. Instead, the XRD pattern resembles

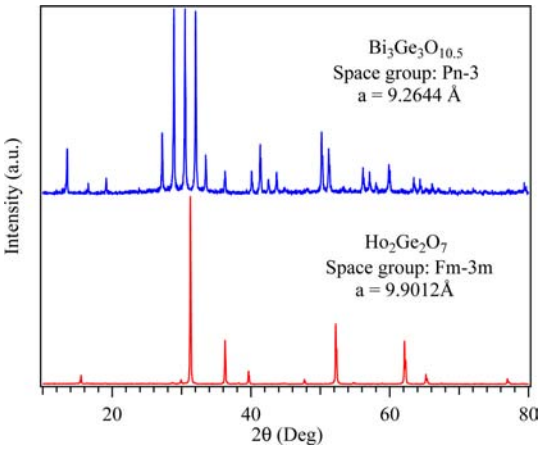

Figure 1. Powder XRD pattern of (a) the high-pressure product with the starting composition "$Bi_2Ge_2O_7$" and (b) the $Ho_2Ge_2O_7$ cubic pyrochlore prepared at 7 GPa and 1000 °C.

those of the $Bi_3Mn_3O_{11\pm\delta}$ samples with the $KSbO_3$-type structure,[11−14] suggesting the formation of a new $KSbO_3$-type "$Bi_3Ge_3O_{10.5}$" phase. To confirm this hypothesis, we have refined its crystal structure from the high-resolution SXRD data in Figure 2a by taking the structure of $Bi_3Mn_3O_{11\pm\delta}$ as a starting structural model,[11−14] which is defined in the cubic $Pn\bar{3}$ space group with two Bi atoms at 24h (x, y, $z = y$) and 4b (0, 0, 0) sites, one Ge position at 12g (x, $^3/_4$, $^1/_4$), and three kinds of oxygen atoms at 8e (x, x, x), 12f (x, $^1/_4$, $^1/_4$), and 24h (x, y, z) sites, respectively. The Bi1 atom at the 24h site with an occupancy factor of $\sim^1/_3$ is found to be disordered. The excellent refinement illustrated in Figure 2a confirmed that the high-pressure product indeed crystallizes into the $KSbO_3$-type cubic structure with lattice parameter a = 9.263 06(1) Å at room temperature. The final atomic coordinates, isotropic thermal, and occupancy factors are presented in Table 1. Selected bond lengths are given in Table 2. A unit-cell crystal structure is displayed in Figure 2b.

The cation ratio Bi:Ge ≈ 1 obtained from the energy dispersive spectroscopy was further confirmed by the Rietveld refinement. Although the refinement on the SXRD cannot provide reliable information about the oxygen stoichiometry, the presence of only Bi^{3+} ions confirmed by X-ray photoelectron spectroscopy in Figure 3 together with the stable Ge^{4+} indicated a chemical formula $Bi_3Ge_3O_{11-\delta}$ with δ = 0.5. In order to distinguish whether the oxygen vacancies are located mainly at the O1 site as in $Bi_3Mn_3O_{10.5}$[12] or distributed randomly at the three oxygen positions, we have refined the SXRD pattern with six different possibilities for distributing oxygen vacancies. As illustrated in Table S1 of Supporting Information, the

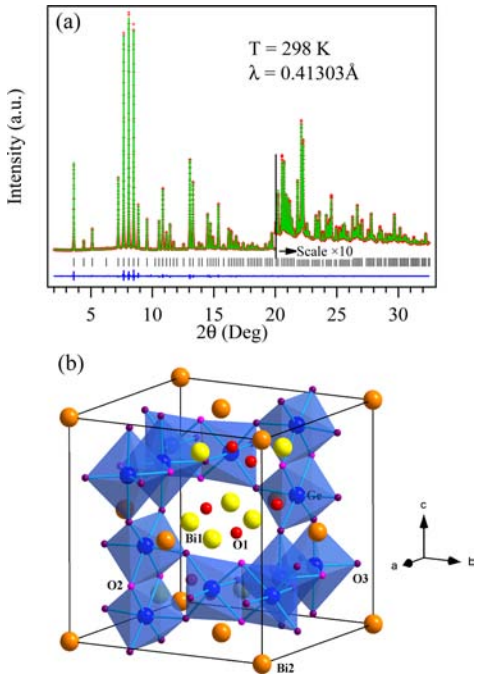

Figure 2. (a) High-resolution SXRD pattern and (b) unit-cell crystal structure of $Bi_3Ge_3O_{10.5}$ after Rietveld refinement.

solution R4, i.e., oxygen vacancies are distributed randomly over all three oxygen positions, is slightly better in terms of the R_{Bragg}.

In contrast to phases commonly found in the Bi−Ge−O system having 4-fold coordinated GeO_4 tetrahedra, the Ge atoms in $Bi_3Ge_3O_{10.5}$ are octahedrally coordinated by oxygen, which is consistent with other oxides containing Ge^{4+} synthesized under high pressure, such as $CaGeO_3$, $SrGeO_3$, and $PbGeO_3$.[15−17] As shown in Figure 2b, the basic units of the crystal structure of $Bi_3Ge_3O_{10.5}$ are edge-shared Ge_2O_{10} octahedral pairs, which are connected to each other via the corner O3 atoms into a three-dimensional framework, characteristic of a cubic $KSbO_3$-related structure. The Bi_6O_3 units are filled into the hexagonal channels formed by the Ge_2O_{10} octahedral units as indicated in Figure 4. The structure was found to be stable down to at least 2 K as shown by the specific-heat data in Figure 5. It seems that the relatively large $\rho = r(Bi^{3+})/r(Ge^{4+})$ = 1.94 is beyond the stability range for the pyrochlore structure in the pressure range below 10 GPa. Higher pressures are required in order to stabilize the pyrochlore structure. In order to accommodate the chemical composition "$BiGeO_{3.5}$", the $KSbO_3$-type structure is one favorable solution under HPHT conditions because it allows the oxygen content to vary from ABO_3 to $ABO_{3.867}$.[12]

As both $Bi_4Ge_3O_{12}$[3,4] and $Bi_{12}GeO_{20}$[5] show useful radio- and photoluminescence (PL), we also performed an initial investigation on the photoluminescence of the new bismuth germanate $Bi_3Ge_3O_{10.5}$. Figure 6 displays the (a) excitation and (b) emission spectra of the $Bi_3Ge_3O_{10.5}$ powder at room temperature. The excitation spectrum in Figure 6a exhibits a strong peak at 375 nm, close to the band gap energy (E_g) of ~3.3 eV, estimated from diffuse reflectance UV−vis spectroscopy. This peak is therefore attributed to the band gap transition. Tauc plot analyses[18] indicate both direct and indirect transitions at the E_g (Figure 7), which is close to that of $Bi_{12}GeO_{20}$ (~3.5 eV[19]) but is smaller than that of $Bi_4Ge_3O_{12}$

dx.doi.org/10.1021/ic3024277 | Inorg. Chem. 2013, 52, 2138−2141

Table 1. Atomic Coordinates and Isotropic Thermal and Occupancy Factors for $Bi_3Ge_3O_{10.5}$ from High-Resolution SXRD[a] at 295 K

atom	site	*x*	*y*	*z*	B_{iso} (Å^2)	occ
Bi1	24h	0.41116(6)	0.37263 (3)	0.37263(3)	1.74(1)	0.34(1)
Bi2	4b	0	0	0	2.42(1)	1.03(1)
Ge	12g	0.40669(8)	0.75	0.25	1.61(2)	1 (fixed)
O1	8e	0.1467(2)	0.1467(2)	0.1467(2)	0.7(1)	0.89(1)
O2	12f	0.6152(4)	0.25	0.25	1.4(1)	0.92(1)
O3	24h	0.5970(3)	0.2495(2)	0.5379(4)	0.61(8)	0.93(1)

[a]Space group $Pn\bar{3}$ (No. 201), a = 9.26309(2) Å, V = 794.817(2) Å^3, Z = 4. Discrepancy factors: R_p = 3.57%, R_{wp}= 5.12%, R_{exp} = 2.30%, χ^2 = 4.93, R_{Bragg} = 1.80%.

Table 2. Selected Bond Lengths (Å) of $Bi_3Ge_3O_{10.5}$ Calculated from Rietveld Refinement

Bi1−O1	2.463(2)	Bi2−O1(×2)	2.354(2)
Bi1−O1(×2)	2.168(2)	Bi2−O3 (×6)	2.505(3)
Bi1−O2	2.480(3)	⟨Bi2−O⟩	2.467
Bi1−O2(×2)	2.926(2)	Ge−O2 (×2)	1.914(3)
Bi1−O3	2.570(3)	Ge−O3 (×2)	1.868(2)
Bi1−O3	2.645(2)	Ge−O3 (×2)	1.965(4)
Bi1−O3	2.984(3)	⟨Ge−O⟩	1.915
⟨Bi1−O⟩	2.593	Ge−Ge	2.899(1)

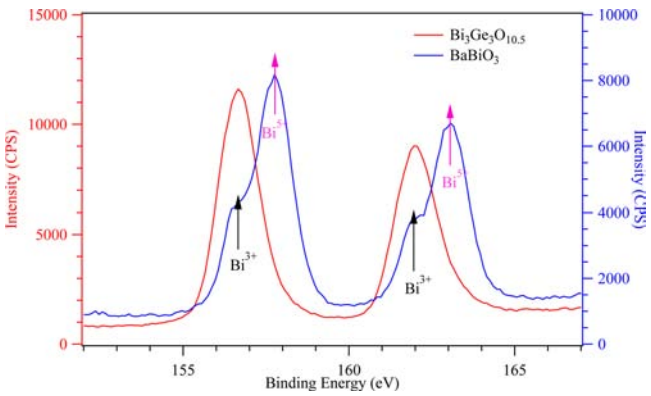

Figure 3. Bi4f XPS spectra of $Bi_3Ge_3O_{10.5}$ and $BaBiO_3$ samples. To probe the valence state of the Bi ions, we measured at room temperature the Bi 4f core-level XPS spectra of $Bi_3Ge_3O_{10.5}$ and compared it to the reference compound, $BaBiO_3$, in which the Bi ions undergo a well-known charge disproportionation reaction: $2Bi^{4+} = Bi^{3+} + Bi^{5+}$. As expected, the double-peak structure of the Bi 4f lines of $BaBiO_3$ confirms the presence of two distinct Bi valence states, i.e., the formal trivalent Bi^{3+} and the pentavalent Bi^{5+}. The component of Bi^{5+} is at higher binding energy than that of Bi^{3+} because of the reduced kinetic energy of outcoming photoelectrons from Bi^{5+} ions due to the larger coulomb attraction. On the other hand, the symmetric Bi 4f spectrum of the $Bi_3Ge_3O_{10.5}$ sample indicates the presence of a single valence state Bi^{3+}.

(~4.5 eV). The emission spectrum shows a collection of peaks ranging from 400 to 600 nm with small Stokes shift of 0.5−1.1 eV, similar to $Bi_{12}GeO_{20}$. Timmermans and Blasse,[20] using $Bi_{12}GeO_{20}$ and Bi_2TiO_{20} powders, concluded that these types of emissions were indicative of radiative recombination in the band gap due to defects and surface states. In contrast, broad emission spectra with large Stokes shifts (>2 eV) (observed in $Bi_4Ge_3O_{12}$, $Bi_2Ge_3O_9$, and $Bi_2Al_4O_9$) were associated with localized transitions on the Bi^{3+} ion. However, a recent study[19] showed intrinsic luminescence in $Bi_{12}GeO_{20}$ single crystals at 450 nm from 8 to 100 K, close to the peak emission in our spectra (Figure 6b). The transition mechanism is still under

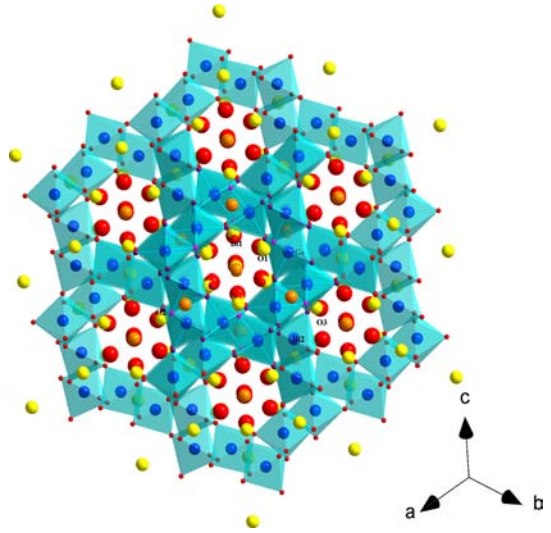

Figure 4. Crystal structure of $Bi_3Ge_3O_{10.5}$ viewed along the [111] direction.

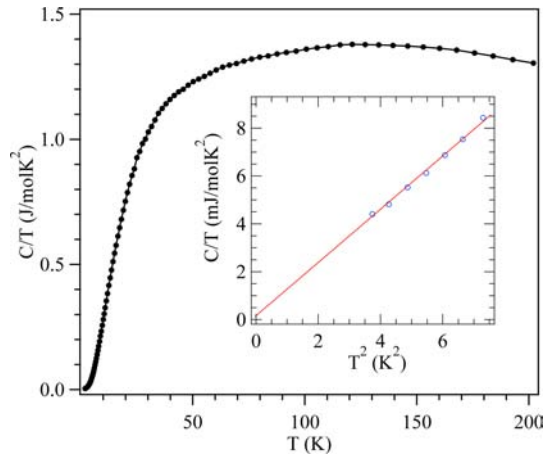

Figure 5. Temperature dependence of the specific heat $C(T)$ of the $Bi_3Ge_3O_{10.5}$ sample in the temperature range from 2 to 200 K. No anomaly was observed in the whole temperature range. The negligible linear term γ derived from the inset plot of C/T vs T^2 is consistent with the insulating state, and the Debye temperature was estimated to be Θ_D = 262 K at low temperature.

debate. Further PL experiments at low temperatures, as well as modeling of the electronic structure of $Bi_3Ge_3O_{10.5}$, are necessary to elucidate the nature of these transitions and represent fascinating areas for future study.

dx.doi.org/10.1021/ic3024277 | Inorg. Chem. 2013, 52, 2138−2141

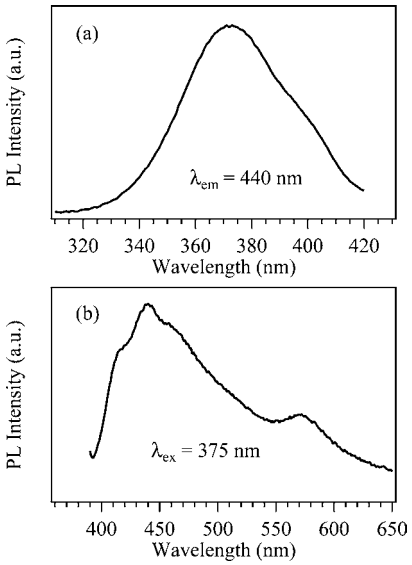

Figure 6. (a) Photoluminescence excitation spectrum with the detector wavelength fixed at 440 nm and (b) emission spectrum using an excitation wavelength of 375 nm for the $Bi_3Ge_3O_{10.5}$ powder sample on quartz at room temperature. The background photoluminescence from a bare quartz substrate has been subtracted.

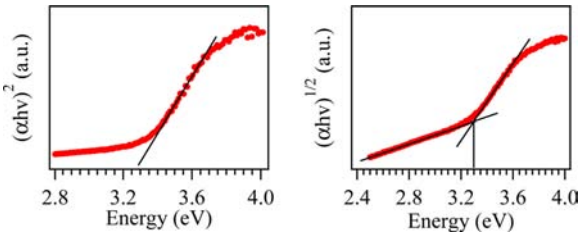

Figure 7. Tauc plots of the diffuse reflectance UV−vis data of $Bi_3Ge_3O_{10.5}$ powder. Transmittance was converted to absorbance by using the formula $A = -\log_{10}(T)$. Tauc plots of $(\alpha hv)^2$ for an allowed direct transition and $(\alpha hv)^{1/2}$ for an allowed indirect transition gave intercepts of ~3.3 eV.

CONCLUSION

In summary, we have prepared a new $KSbO_3$-type bismuth germanate $Bi_3Ge_3O_{10.5}$ under 7 GPa and 700 °C and determined its crystal structure via Rietveld refinement on the high-resolution SXRD data. The photoluminescence emission spectrum at room temperature exhibits a complex structure in the range from 400 to 600 nm. A band gap of ca. 3.3 eV was estimated from the UV−vis spectra.

ASSOCIATED CONTENT

Supporting Information

Additional table. This material is available free of charge via the Internet at http://pubs.acs.org.

AUTHOR INFORMATION

Corresponding Author

*E-mail: jgcheng@utexas.edu (J.C.); jszhou@mail.utexas.edu (J.Z.).

Present Address

[∇]Institute of Physics, Chinese Academy of Science, Beijing 100190, China.

Notes

The authors declare no competing financial interest.

ACKNOWLEDGMENTS

This work was supported by NSF MIRT (DMR-1122603) and the Robert A. Welch Foundation (Grant F-1066). Use of the Advanced Photon Source at Argonne National Laboratory was supported by the U.S. Department of Energy, Office of Science, Office of Basic Energy Sciences, under Contract DE-AC02-06CH11357. The work at ORNL was supported by the U.S. Department of Energy, Basic Energy Sciences and Engineering Division. We gratefully acknowledge C. Jackson Stolle and Brian A. Korgel for their help with diffuse reflectance UV−vis spectroscopy measurements.

REFERENCES

(1) Speranskaya, E. I.; Arshakuni, A. A. *Russ. J. Inorg. Chem.* **1964**, *9*, 226.
(2) Kaplun, A. B.; Meshalkin, A. B. *J. Cryst. Growth* **1996**, *167*, 171−175.
(3) Weber, M. J.; Monchamp, R. R. *J. Appl. Phys.* **1973**, *44*, 5495.
(4) Dieguez, E.; Arizmendi, L.; Cabrera, J. M. *J. Phys. C: Solid State Phys.* **1985**, *18*, 4777.
(5) Lauer, R. B. *Appl. Phys. Lett.* **1970**, *17*, 178.
(6) Cheng, J.-G.; Zhou, J.-S.; Goodenough, J. B. *Phys. Rev. B* **2010**, *81*, 134412.
(7) Wang, J.; Toby, B. H.; Lee, P. L.; Ribaud, L.; Antao, S.; Kurtz, C.; Ramanathan, M.; von Dreele, R. B.; Beno, M. A. *Rev. Sci. Instrum.* **2008**, *79*, 085105.
(8) Toby, B. H. *J. Appl. Crystallogr.* **2001**, *34*, 210−213.
(9) Brisse, F.; Knop, O. *Acta Crystallogr., Sect. A* **1966**, *21*, 44.
(10) Ried, A. F.; Li, C.; Ringwond, A. E. *J. Solid State Chem.* **1977**, *20*, 219.
(11) Belik, A. A.; Takayama-Muromachi, E. *J. Am. Chem. Soc.* **2009**, *131*, 9504.
(12) Belik, A. A.; Takayama-Muromachi, E. *J. Am. Chem. Soc.* **2010**, *132*, 12426−12432.
(13) Valant, M.; Babu, G. S.; Vrcon, M.; Kolodiazhnyi Axelsson, A.-K. *J. Am. Chem. Soc.* **2012**, *95*, 644.
(14) Li, M.-R; Retuerto, M.; Go, Y. B.; Emge, T. J.; Croft, M.; Ignatov, A.; Ramanujachary, K. V.; Dachraoui, W.; Hadermann, J.; Tang, M.-B.; Zhao, J.-T.; Greenblatt, M. *J. Solid State Chem.* **2013**, *197*, 543.
(15) Sasaki, S.; Prewitt, C. T.; Liebermann, R. C. *Am. Mineral.* **1983**, *68*, 1189.
(16) Akaogi, M.; Kojitani, H.; Yusa, H.; Yamamoto, R.; Kido, M.; Koyama, K. *Phys. Chem. Miner.* **2005**, *32*, 603.
(17) Xiao, W.; Tan, D.; Zhou, W.; Chen, M.; Xiong, X.; Song, M.; Liu, J.; Mao, H.-K.; Xu, J. *Am. Mineral.* **2012**, *97*, 1193.
(18) Chen, Z.; Jaramillo, T. F.; Deutsch, T. G.; et al. *J. Mater. Res.* **2010**, *25*, 3−16.
(19) Itoh, M.; Katagiri, T. *J. Phys. Soc. Jpn.* **2010**, *79* (7), 074717.
(20) Timmermans, C. W. M.; Blasse, G. *J. Solid State Chem.* **1984**, *52*, 222−232.